



## Latent ruthenium initiators containing fluoro aryloxy ligands

Zhanru Yu<sup>a,1</sup>, Yulia Rogan<sup>a,2</sup>, Ezat Khosravi<sup>a,\*</sup>, Osama M. Musa<sup>b,3</sup>, Lois Hobson<sup>c,4</sup>, Andrei S. Batsanov<sup>a</sup>

<sup>a</sup>Durham University, Chemistry Department, South Road, Durham DH1 3LE, UK

<sup>b</sup>International Specialty Products (ISP), 1361 Alps Road, NJ07470, USA

<sup>c</sup>ICI, STG, Wilton, Teesside, UK

### ARTICLE INFO

#### Article history:

Received 18 October 2010

Received in revised form

20 December 2010

Accepted 11 January 2011

#### Keywords:

Thermally switchable ruthenium initiators

Ring opening metathesis polymerization (ROMP)

Norbornene dicarboximides

Latent catalysts

### ABSTRACT

A new ligand, methyl 2,3,5,6-tetrafluoro-4-oxybenzoate ( $C_8H_3F_4O_3$ ), combining an electron withdrawing group ( $C_6F_4$ ) to tune the reactivity with an anchor group ( $CO_2Me$ ) for immobilization on supports, was used to prepare four new ruthenium initiators, viz.  $Ru(C_8H_3F_4O_3)_2(=CHPh)(3-Br-C_5H_5N)(H_2IMes)$  and  $Ru(C_8H_3F_4O_3)_2XL$ , where  $X = C, N-(=CHCH_2CH_2-2-C_5H_4N)$  and  $L = P^tPr_3, PCy_3$  or  $H_2IMes$ . The new ligand greatly reduced the reactivity of the ruthenium centre at room temperature. The  $^1H$  NMR and DSC investigation for the ROMP of norbornene dicarboximide monomers clearly demonstrated that the  $Ru(C_8H_3F_4O_3)_2XL$  initiators were inactive at room temperature and required elevated temperatures for their activation.

© 2011 Elsevier B.V. All rights reserved.

### 1. Introduction

Ring opening metathesis polymerization (ROMP) using well-defined initiators based on molybdenum [1–5] and ruthenium [6–10] is now well-established as a powerful polymerization tool allowing the synthesis of materials with desired properties [8,11–17]. These well-defined initiators polymerize norbornene and its derivatives efficiently at room temperature. However, for some processes, it is desirable to control the initiation step in order to allow adequate mixing of monomer and initiator before polymerization occurs. For these applications, complexes that are inactive at room temperature and initiate polymerization only upon heating would be desirable. Development of well-defined latent ruthenium initiators considerably expands the range of applications, particularly in industry. The latent initiators allow storing, transporting and polymerizing materials at desirable temperatures. During the last few years efforts have been focused

on the search for effective thermally switchable ruthenium complexes suitable for ROMP of norbornene monomers [17–28].

Related to the work presented here, Ciba reported initiators **1a–f** (Fig. 1) which were claimed to be inactive at room temperature but active at elevated temperatures for the polymerization of dicyclopentadiene (DCPD) [18,19,29]. At the fixed polymerization temperature of 60 °C, both complexes **1b** and **1f** showed the onset temperatures of 40 °C with the exotherms reaching 165 °C and 180 °C, respectively, within 2 min. Only **1a** polymerized DCPD at 90 °C and with an exotherm at 120 °C.

Initiators **2a–c** containing  $H_2IMes$  ligand (Fig. 1) instead of  $^tPr_3P$  ligand were also reported [20]. ROMP of DCPD using **2a**, showed an exotherm within 3 min at 30 °C. The complexes **2c** and **2b** were reported to have similar behaviour to **2a**. For ROMP of DCPD with complex **3a**, an exotherm was observed after 1 min at 30 °C [21]. For initiators **3b** and **3c**, under similar conditions, the introduction of  $^iPr$  and  $Cy$  (Cyclohexyl) groups on the nitrogen atom resulted in the appearance of exotherms after 18 and 28 min at 30 °C, respectively [21]. These results indicate the unsuitability of these initiators as latent. Moreover, it should be noted that the thermal switchability of the initiators **1–3** has not been investigated for ROMP of functionalized norbornene monomers.

The characteristics of the ligands in ruthenium initiators play a crucial role in their overall activity, particularly in ROMP of norbornene derivatives. The chelation effect [18,19,29–35] and the presence of electron withdrawing and electron donating groups in ligands surrounding Ru centre [27,36–41] can influence the

\* Corresponding author. Tel.: +44 191 334 2014; fax: +44 191 334 2051.

E-mail address: [ezat.khosravi@durham.ac.uk](mailto:ezat.khosravi@durham.ac.uk) (E. Khosravi).

<sup>1</sup> Present address: The Weatherall Institute of Molecular Medicine, University of Oxford, Headington, Oxford OX3 9DS, UK.

<sup>2</sup> Present address: School of Chemistry, Cardiff University, Cardiff CF10 3XQ, UK.

<sup>3</sup> Previous address: Henkel Corporation, Bridgewater, NJ, USA.

<sup>4</sup> Present address: Centre for Process Innovation, Wilton Centre, Teesside TS10 4RF, UK.

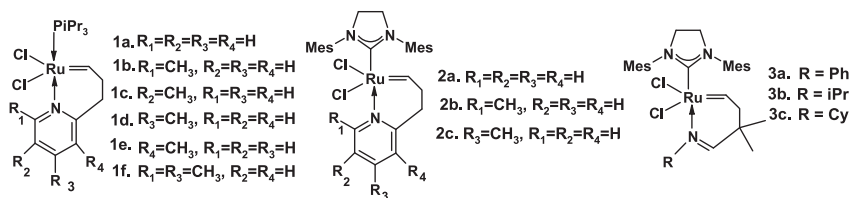


Fig. 1. Previous examples of ROMP catalysts containing N-chelating alkylidene ligands.

behaviour of the ruthenium initiators in ROMP of norbornene derivatives.

The synthesis and activity of ruthenium complexes containing perfluorophenoxide ligand (**4**) or perbromophenoxide ligand (**5**) (Fig. 2) were reported and they were shown to be efficient initiators for ROMP of cyclooctene and norbornene monomers at room temperature, with the rate of propagation being faster than that of the initiation [36–39].

It is generally accepted that in the case of the first generation,  $RuCl_2(=CHPh)(PCy_3)_2$ , and also second generation,  $RuCl_2(=CHPh)(PCy_3)(H_2IMes)$ , Grubbs ruthenium initiators dissociation of the donor ligand ( $PCy_3$ ) is necessary to start the ROMP reaction [42]. In contrast, for oxygen chelated Grubbs–Hoveyda type complexes, it is believed that initially 14-electron intermediate is formed through the dissociation of the benzylidene ether chelating group [33,43]. Coordination of the alkene substrate, followed by metathesis, would then lead to the formation of the catalytically active species and a molecule of isopropoxy styrene. When the olefin is completely consumed, the catalyst is then believed to return to its resting state by re-binding the isopropoxy styrene (release/return mechanism). The dissociation mechanism for Hoveyda–Grubbs complexes and the influence of substituents on the benzene ring on Ru–O bond length and hence on alkoxy-dissociation have also been investigated [34,35]. Recently, both dissociation and association mechanism as interchange mechanism have been reported for olefin metathesis involving Grubbs–Hoveyda and Grela type complexes, however, it was difficult to decide which mechanism was dominant [44].

It should be noted that these studies concern oxygen chelated complexes and to the best of our knowledge there are no reports of either dissociative or associative mechanisms for nitrogen chelated complexes. For the ruthenium complexes **1–3**, the dissociation of chelating nitrogen to the metal centre is believed to be necessary for initiating the ROMP reaction. This dissociation readily takes place at room temperature, in the presence of a monomer, making the initiator active for ROMP. Therefore, the dissociation process, at room temperature, must be slowed down or even prevented in order to render these ROMP initiators latent.

We recently started a programme of work to develop a series of thermally switchable ruthenium initiators for various applications. Herein, we describe the synthesis of the designed ligand **6**, methyl 2,3,5,6-tetrafluoro-4-oxybenzoate, and the new ruthenium initiators **7–10** containing ligand **6**, Fig. 3. The design of the ligand **6** is novel and is based on the incorporation of an electron withdrawing group ( $-C_6F_4$ ) and an anchor group ( $-CO_2Me$ ). The electron withdrawing nature of  $-C_6F_4$  group is expected to make the nitrogen–ruthenium chelation stronger and therefore rendering these ruthenium initiators less reactive at room temperature. The anchor group is to provide the means for immobilization of the initiators on Merrifield-type supports for combinatorial processes. The immobilization process is not presented here and it will be the subject of the future publications. However, the proposed process for the immobilization would involve the conversion of carboxylic functional groups, on Merrifield-type resin, to diamine by the

reaction with Boc-protected diaminodiethylamine followed by a deprotection reaction. The reaction of amine functional groups with 2,3,5,6-tetrafluoro-4-aceto benzoic acid would be followed by the conversion of the acetate groups to hydroxyl groups. The hydroxyl groups would then be reacted with thallium ethoxide to form thallium salt of ligand **6** (**TI-6**) which upon reactions with appropriate ruthenium complexes would be anticipated to lead to immobilized ruthenium initiators **7–10**.

## 2. Results and discussions

### 2.1. Synthesis of the ligand **6**

The ligand **6** was prepared by a two-step procedure shown in Scheme 1. The esterification reaction of 2,3,5,6-tetrafluoro-4-hydroxybenzoic acid hydrate in methanol in the presence of concentrated sulphuric acid gave white solid intermediate product, methyl 2,3,5,6-tetrafluoro-4-hydroxybenzoate, in high yield (90%). The reaction of the intermediate product with thallium ethoxide in anhydrous THF gave the white solid product, the thallium salt of **6** (**TI-6**), in high yield (90%). The structures of the intermediate product and **TI-6** were confirmed by  $^1H$ ,  $^{13}C$  and  $^{19}F$  NMR.

### 2.2. Synthesis and characterization of the new ruthenium initiators **7–10**

The new ruthenium initiator **7** was prepared via exchange reactions between ruthenium complex **1a** and two equivalents of **TI-6**, Scheme 2. The course of the ligand exchange reaction was followed by  $^1H$  NMR. Disappearance of the alkylidene proton resonance at 19.40 ppm and appearance of a new alkylidene proton resonance at 19.86 ppm indicated the complete conversion of complex **1a** to **7**, which was characterized by single-crystal X-ray diffraction, Fig. 4. The Ru coordination is square-pyramidal with C (39) in the apical position and the fluorophenoxide ligands trans to each other. Thus **7** can be regarded as an analogue of **1a** [18] with both chloro ligands replaced by fluorophenoxide ligands. The O (1)–Ru–O(2) angle of  $148.2(1)^\circ$  is smaller than P–Ru–N(1) of  $173.58(7)^\circ$ , indicating a distortion towards trigonal-bipyramidal

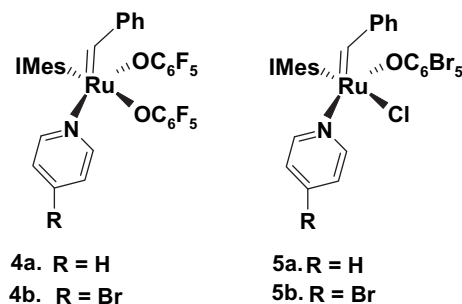


Fig. 2. Structures of ruthenium initiators with two  $-OC_6F_5$  (**4**) and one  $-OC_6Br_5$  (**5**) ligands.

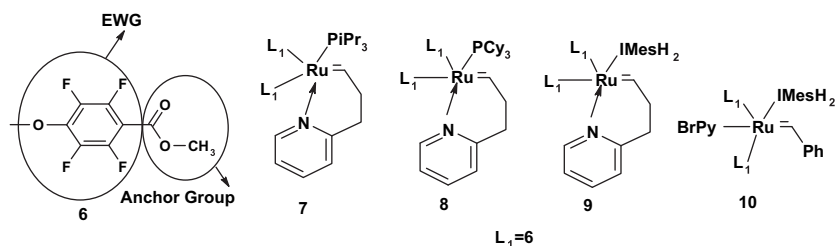


Fig. 3. The structures of the new ligand **6** and the new ruthenium initiators **7–10**.

coordination stronger than in **1a** (Cl–Ru–Cl 155.27(3) and P–Ru–N 172.80(6)°).

The new ruthenium initiator **8** could not directly be obtained from **7**. Therefore, initially complex **11** was obtained by two routes outlined in Scheme 2. Either the ruthenium complex **1a** was reacted with an excess of tricyclohexylphosphine or Grubbs first generation ruthenium complex **12** was reacted with an excess of **13** to give (in both cases) complex **11**, which was then converted into the new ruthenium initiator **8** by treatment with two equivalents of **TI-6**. In the <sup>1</sup>H NMR spectrum, the resonance due to the proton of the alkylidene moiety was observed at 19.91 ppm. Attempts to prepare crystals of **8** suitable for X-ray analysis were unsuccessful.

The synthetic route to the new ruthenium initiator **9** is shown in Scheme 3. The ruthenium complex **14** [20] was reacted with 2 equivalents of **TI-6** to give **9**. In the <sup>1</sup>H NMR spectrum of **9** the corresponding resonance due to the proton of the alkylidene moiety was observed at 19.47 ppm. Attempts to prepare high quality crystals of **9** for X-ray analysis were unsuccessful.

The ligand exchange reactions of the first generation (**12**) and also the second generation Grubbs ruthenium complexes with **TI-6**, either in toluene or in THF, gave no new initiators, as indicated by <sup>1</sup>H NMR investigations.

The new ruthenium initiator **10** was prepared via exchange reactions between the bromopyridine modified second generation ruthenium complex **15** and 2 equivalents of **TI-6**, Scheme 3. Disappearance of the alkylidene proton resonance at 19.40 ppm and appearance of a new alkylidene proton resonance at 18.77 ppm indicated the complete conversion of complex **15**–**10**. The latter, in the form of **10**·½CH<sub>2</sub>Cl<sub>2</sub> solvate (crystals grown from a mixture of dichloromethane and hexane) was characterized by single-crystal X-ray diffraction (Fig. 5, Table 1). The asymmetric unit comprises two molecules, *A* and *B*, besides one disordered molecule of dichloromethane. The Ru atom has a distorted square-pyramidal coordination, with the apical benzylidene ligand and the basal positions occupied by the H<sub>2</sub>IMes, bromopyridine and two fluoro-phenoxide ligands in *cis* arrangement. The conformations of molecules *A* and *B* differ significantly (Fig. 5). As usual [45], steric overcrowding causes an overall tilt of the H<sub>2</sub>IMes ligand towards the vacant coordination site of the Ru (which is located *trans* to the benzylidene ligand), as indicated by the unsymmetrical Ru–C(2)–N angles. In molecule *B*, the (mesityl) methyl group C(17)H<sub>3</sub> provides an agostic Ru...H interaction at this site. The Ru'...H(176) distance of 2.61(3) Å for the refined and 2.56 Å for the idealised (assuming C–H distance of 1.08 Å) hydrogen position, is substantially shorter

than the sum of van der Waals radii (2.17 Å [46] to 2.05 Å [47] for Ru and 1.10 Å for H [48]). However, the corresponding Ru...H distance in molecule *A* is 0.46 Å longer. In molecule *B*, the bromopyridine ligand is disordered by a ca. 180° rotation around the Ru'–N(2') bond [i.e. the bromine atom is disordered between two positions, Br(1') and Br(2')], in a 93:7 ratio; the *minor* orientation is identical with the *only* orientation observed in molecule *A*. In both molecules the apical benzylidene ligand shows a small twist (16.1° in *A*, 15.1° in *B*) between the Ru=C(20) bond and the phenyl ring which has a staggered orientation between the bromopyridine and a fluoro-phenoxide ligands.

Thus, **10** has the same coordination geometry as **4a** [36] (Table 1) but a rather different molecular conformation. In **10**, the pyridine ring is stacked with the N(1)-bonded mesityl group (dihedral angles 7.5° in *A*, 17.9° in *B*). Interestingly, although the two fluoroarene rings are oriented differently in molecules *A* and *B*, in both they are stacked face-to-face with small interplanar angles of 11.9° (*A*) or 8.9° (*B*). In **4a**, the pyridine/mesityl stacking is only marginal, and that between perfluoroarenes is absent altogether. In **10**, as in **4a**, the Ru–O bond opposing the H<sub>2</sub>IMes ligand is substantially longer than that opposing the bromopyridine ligand, in accordance with the relative *trans* influence of these ligands. However, the effect is much smaller than in an octahedral complex, *t*-BuC=C=RuCl<sub>2</sub>(bipy)(H<sub>2</sub>IMes) [49], where the Ru–Cl bonds opposite to Ru–C(H<sub>2</sub>IMes) and Ru–N(bipy) measure 2.49 and 2.39 Å, respectively.

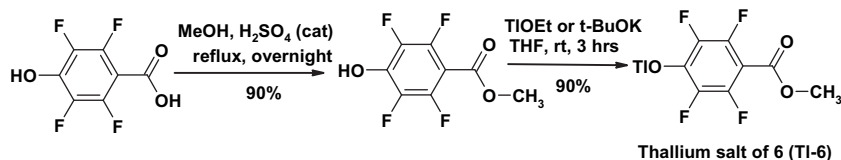
### 2.3. Stability of the new ruthenium initiators **7–10**

The new ruthenium initiators **7–10** were dissolved in CDCl<sub>3</sub> in sealed NMR tubes, kept at 50 °C and <sup>1</sup>H NMR spectra were taken at different intervals over the period of up to 24 h. The investigation revealed no detectable decrease in the intensity of the alkylidene protons. This indicated the stability of these initiators in solution at 50 °C, over the times-scale of the ROMP reactions.

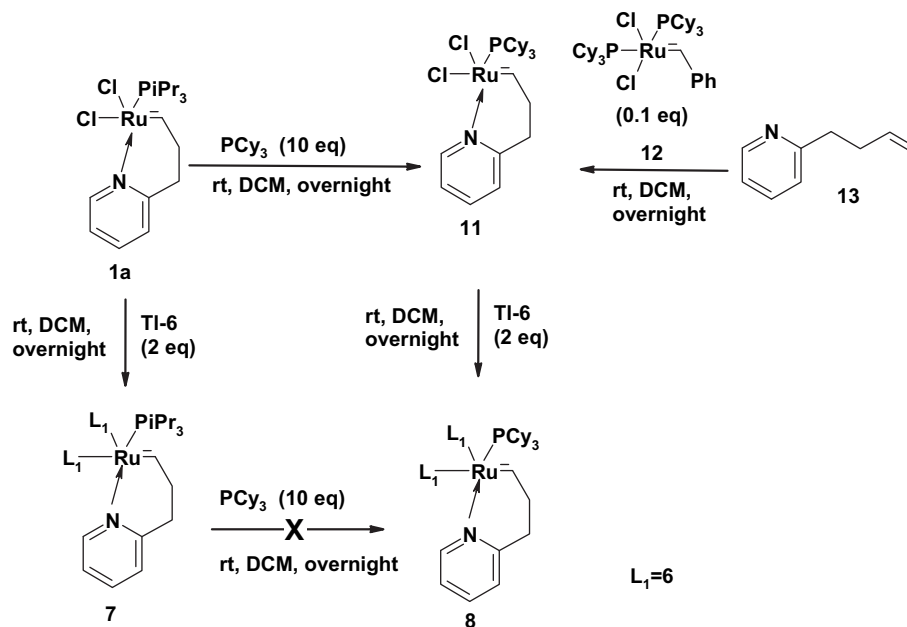
### 2.4. Thermal switchability of the new ruthenium initiators **7–10** in ROMP

#### 2.4.1. Investigation by <sup>1</sup>H NMR analysis

The reactivity and thermal switchability of the new ruthenium initiators **7–10** for ROMP of norbornene dicarboximide monomers, shown in Fig. 6, were investigated by <sup>1</sup>H NMR and the results are summarised in Table 2. The ROMP reactions, under similar



Scheme 1. Preparation of the thallium salt of the ligand **6** (**TI-6**).



Scheme 2. Preparation route for the new ruthenium complexes 7 and 8.

conditions, were also carried out on these monomers using ruthenium complex **1a** to provide comparison. The conversions of monomers to polymers were determined by comparing the integration of the vinylic protons of monomers at 6.30 ppm to that of the polymers at 5.75 ppm in the  $^1\text{H}$  NMR spectra of the ROMP reaction mixtures. The error in the integration was dependent on the amount of unreacted monomer present in the mixture and it is estimated to be about 10%.

The  $^1\text{H}$  NMR spectrum of the reaction mixture for the ROMP of N-2-ethylhexyl norbornene dicarboximide (2EHNB) monomer using initiator **7** showed no detectable conversion of monomer to polymer after 1 h (Fig. 7a) and a conversion of 3% after 24 h (Fig. 7b), at room temperature. However, a conversion of 80% was observed after 24 h at 55 °C (Fig. 7c). Similar results were obtained for the ROMP of other norbornene dicarboximide monomers, shown in Fig. 6, using initiator **7** under similar conditions (Table 2).

The ROMP of norbornene dicarboximide monomers with initiator **8**, under similar condition, gave the same results to those for initiator **7**, Table 2.

The  $^1\text{H}$  NMR spectra of the reaction mixture for the ROMP of N-hexyl norbornene dicarboximide (HNB) monomer using initiator **9** showed a conversion of monomer to polymer of 6% after 1 h at room temperature, Fig. 8a. However, conversions of 38% and 95% were obtained after 6 h and 24 h, respectively, at 55 °C, Fig. 8b, c.

Initiator **10** was found to be an efficient initiator for the ROMP of norbornene dicarboximide monomers at room temperature, based on solution  $^1\text{H}$  NMR results. The  $^1\text{H}$  NMR spectra of the reaction mixture for the ROMP of 2EHNB, HNB and N-decyl norbornene dicarboximide (DecNB) monomers with initiator **10** showed conversions of monomer to polymer of 99% after 24 h at room temperature.

The solution  $^1\text{H}$  NMR results showed that the new ruthenium complexes **7–10** were good initiators for ROMP of norbornene dicarboximide monomers. Moreover, it was established that initiators **7** and **8** were inactive ROMP initiators at room temperature giving conversion of monomers to polymers of less than 5% after

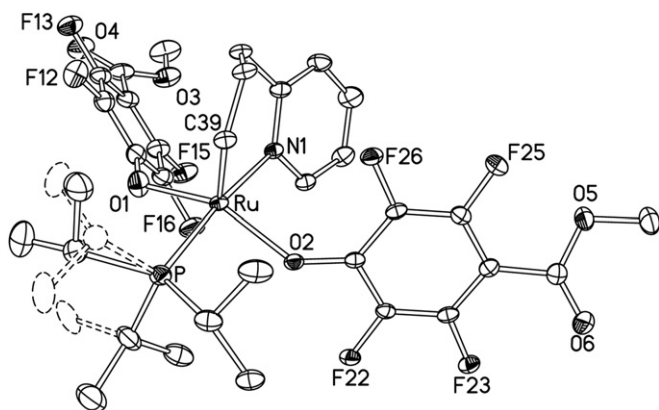
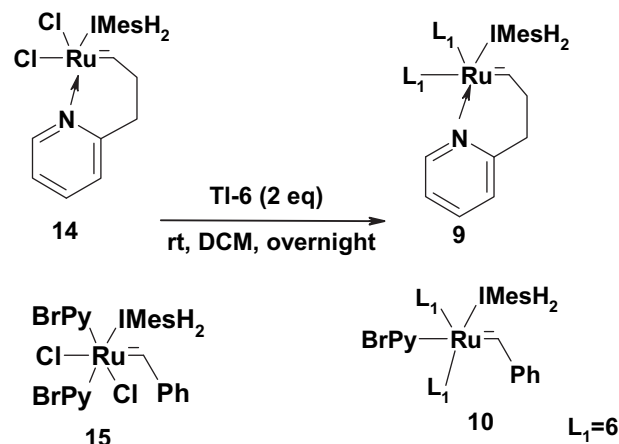


Fig. 4. X-ray molecular structure of new ruthenium initiator **7** (thermal ellipsoids at the 30% probability, H atoms omitted), showing the disorder of *i*-Pr groups. Selected bond distances (Å) and angles (°): Ru–P 2.3317(9), Ru–O(1) 2.019(2), Ru–O(2) 2.015(2), Ru–N(1) 2.157(2), Ru=C(39) 1.821(3), C(39)–Ru–P 93.5(1), C(39)–Ru–O(1) 104.0(1), C(39)–Ru–O(2) 107.7(1), C(39)–Ru–N(1) 91.65(12), O(1)–Ru–O(2) 148.2(1), P–Ru–N(1) 173.58(7).



Scheme 3. Synthesis route for the new ruthenium initiators **9** and **10**.

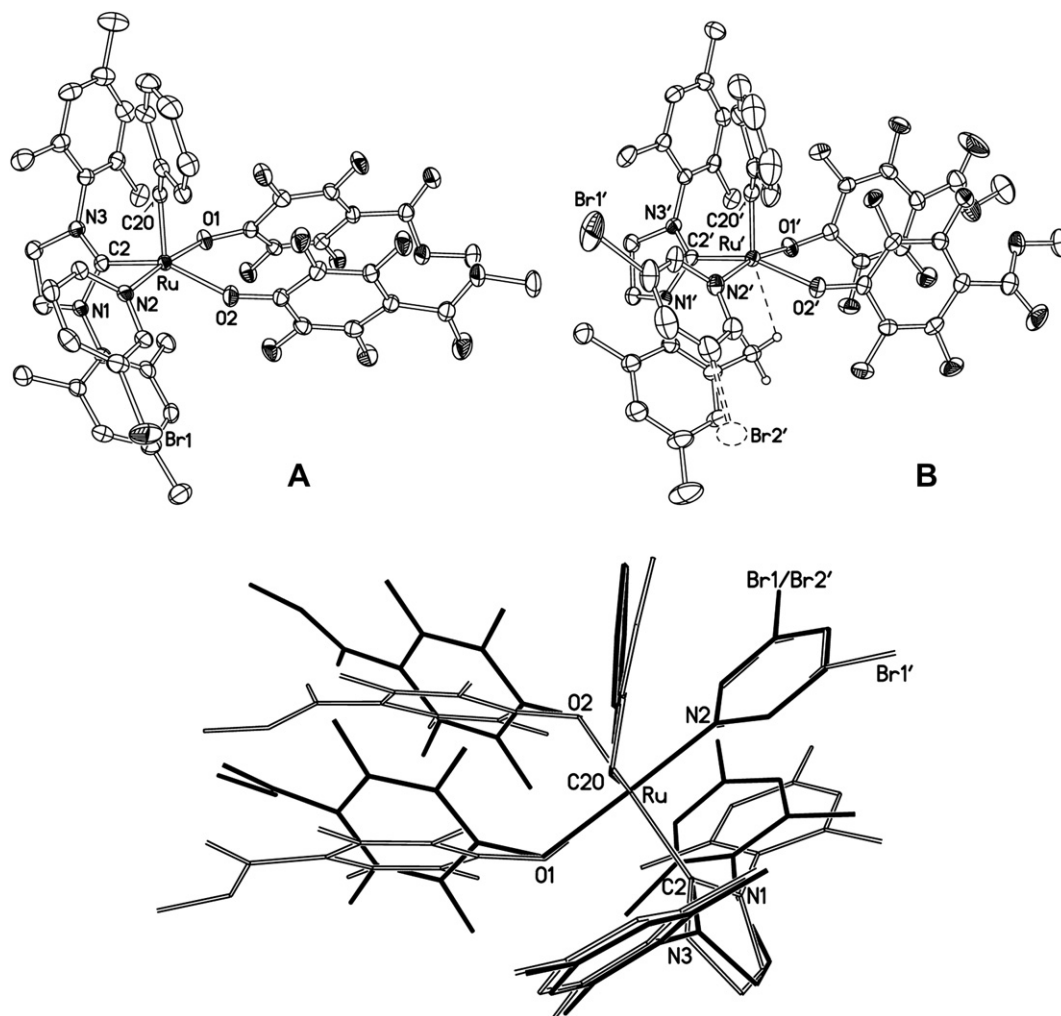


Fig. 5. Independent molecules A and B in the crystal of  $10 \cdot \frac{1}{2} \text{CH}_2\text{Cl}_2$  (thermal ellipsoids at 50% probability, hydrogen atoms omitted) and their superposition (A dark, B light).

24 h and that they required elevated temperatures for their activation. We believe this is due to the electron withdrawing nature of the ligand **6** which strengthens the chelation of nitrogen to the ruthenium centre. Therefore, elevated temperatures are necessary to overcome the chelation and hence initiate ROMP reactions. It should be noted that the ROMP of these monomers using initiator **1a**, which was reported to be latent for the ROMP of DCPD, gave conversions of 99% after 24 h at room temperature. This clearly showed that the initiator **1a** is active at room temperature and

**Table 1**  
Selected bond distances (Å) and angles ( $^\circ$ ) in **10** and **4a**.

	<b>10</b> , mol. A	<b>10</b> , mol. B	<b>4a</b>
Ru–O(1)	2.094(2)	2.089(2)	2.110(3)
Ru–O(2)	2.063(2)	2.074(2)	2.076(3)
Ru–N(2)	2.073(2)	2.060(2)	2.085(3)
Ru–C(2)	2.027(2)	2.029(2)	2.040(4)
Ru=C(20)	1.834(2)	1.836(3)	1.843(3)
C(20)–Ru–O(1)	89.17(9)	96.25(10)	96.7(1)
C(20)–Ru–O(2)	109.87(9)	104.45(9)	103.1(1)
C(20)–Ru–N(2)	95.46(9)	94.4(1)	92.6(1)
C(20)–Ru–C(2)	96.6(1)	98.0(1)	91.2(1)
O(1)–Ru–N(2)	174.87(7)	169.06(8)	171.2(1)
O(2)–Ru–C(2)	153.52(8)	157.52(8)	164.0(1)
Ru–C(2)–N(1)	117.5(2)	120.4(2)	127.6(2)
Ru–C(2)–N(3)	135.1(2)	132.0(2)	130.5(2)

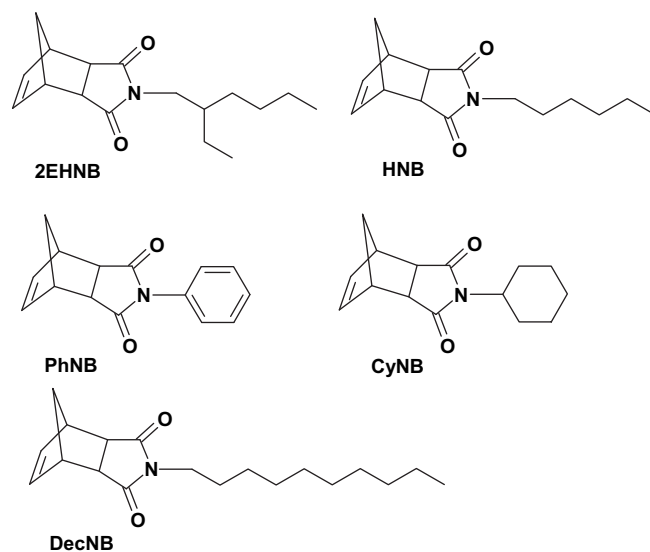


Fig. 6. Structures of the norbornene dicarboximide monomers.

**Table 2**  
The ROMP of norbornene dicarboximide monomers with the new ruthenium initiators **7–10** and **1a**.

Monomer	Initiators <b>7</b> and <b>8</b>		Initiator <b>9</b>		Initiator <b>10</b>	<b>1a</b>
	% Conversion		% Conversion		% Conversion	% Conversion
	RT	55 °C	RT	55 °C	RT	RT
	24 h	24 h	1 h	24 h	24 h	24 h
2EHNB	3	80	8	95	99	99
HNB	2	85	6	95	99	99
DecNB	3	86			99	99
CyNB	2	78				99
PhNB	4	79				99

therefore it is not a thermally switchable initiator for ROMP of functionalized norbornene monomers.

#### 2.4.2. Investigation by DSC analysis

The thermal switchability of the new ruthenium initiators **7** and **8** for the ROMP reactions, in bulk, of norbornene dicarboximide monomers was further investigated by DSC analysis and the results are shown in Table 3. The DSC studies were only performed on 2EHNB and HNB monomers as they were liquid monomers allowing ROMP reactions in bulk.

The DSC thermographs for the ROMP of 2EHNB monomer using initiator **7** are shown in Fig. 9. When the DSC was run at 20–300 °C at 10 °C/min, an exotherm peak was observed with a maximum at 135 °C along with an endotherm peak at 210 °C, Fig. 9a. The analysis of the retrieved sample after running DSC revealed a conversion of monomer to polymer of 90%. The DSC analysis of the neat 2EHNB monomer, run under the same conditions, showed an endotherm at about 200 °C due to a retro Diels–Alder reaction, Fig. 9b. Therefore, the endotherm peak in Fig. 9a was attributed to the retro Diels–Alder of the unreacted monomer. Initiator **7** was deactivated to such an extent, due to the presence of ligand **6**, that the ROMP reactions were slow. Therefore, on the time-scale of the DSC runs the conversion of monomer to polymer was not complete and the unreacted monomer went through a retro Diels–Alder reaction.

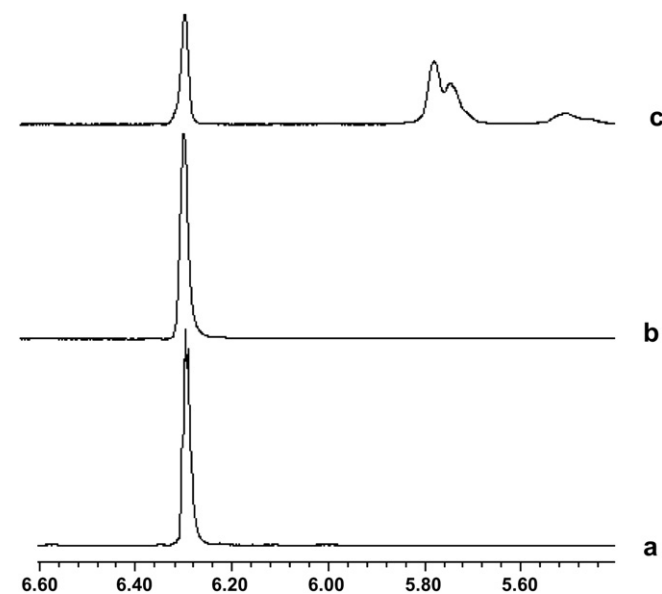


**Fig. 7.**  $^1\text{H}$  NMR spectra of the vinylic region for ROMP of 2EHNB monomer with the new ruthenium initiator **7**; a) at room temperature after 1 h; b) at room temperature after 24 h; c) at 55 °C after 20 h.

When the DSC was run and the temperature was kept at 180 °C for 30 min, complete conversion of monomer to polymer was achieved and no endotherm was observed, Fig. 9c. The Fig. 9c clearly shows that no polymerization was observed at room temperature and that the polymerization started at 75 °C with an exotherm peak maximum at 127 °C. The DSC thermograph for the ROMP of HNB monomer using initiator **8**, showed no sign of polymerization at room temperature and that the polymerization started at 60 °C with an exotherm peak maximum at 100 °C (Fig. 10). The  $^1\text{H}$  NMR spectrum of the polymerization mixtures retrieved from the DSC pans after the DSC measurements revealed that complete conversions of monomers to polymers were achieved in all cases.

In contrast to results obtained for initiators **7** and **8**, the DSC thermograph for the ROMP of HNB monomer using ruthenium complex **1a** showed that the polymerization started at 40 °C with an exotherm peak maximum at 55 °C. This further confirmed the unsuitability of **1a** as a thermally switchable initiator, as it was shown by the  $^1\text{H}$  NMR investigations.

The DSC investigation results for the ROMP of norbornene dicarboximide monomers clearly confirmed the results obtained by  $^1\text{H}$  NMR that the new ruthenium initiators **7** and **8** were inactive at room temperature and that they required elevated temperatures for their activation.

### 3. Conclusions

The new ligand **6** was designed to incorporate an electron withdrawing group ( $-\text{C}_6\text{F}_4$ ) group to tune the reactivity of the ruthenium initiators and an anchor group ( $-\text{CO}_2\text{Me}$ ) for immobilization of the ruthenium initiators on supports. The ligand **6** was prepared in high yield and its structure was confirmed by  $^1\text{H}$ ,  $^{13}\text{C}$  and  $^{19}\text{F}$  NMR.

A new range of ruthenium initiators, **7–10**, were prepared bearing the new ligand **6**; two of these (**7** and **10**) were characterized by single-crystal X-ray diffraction.

The  $^1\text{H}$  NMR investigation results for the ROMP of norbornene dicarboximide monomers clearly demonstrated that initiators **7** and **8** were inactive for ROMP at room temperature giving conversions of monomer to polymer of less than 5% after 24 h but became active at elevated temperatures giving high conversions. It was also found that initiator **9** was more active than initiators **7** and **8** and that initiator **10** was active for ROMP at room temperature.

The results of  $^1\text{H}$  NMR and DSC investigations for the ROMP of norbornene dicarboximide monomers clearly demonstrated that the new ruthenium initiators **7** and **8** were inactive at room temperature and that they required elevated temperatures for their activation, due to the increased strength of chelation of nitrogen to the ruthenium centre upon the inclusion of ligand **6**.

These observations confirmed the new ruthenium initiators **7** and **8** as excellent thermally switchable ruthenium initiators.

### 4. Experimental section

#### 4.1. General

All reactions involving metal complexes were conducted in oven-dried glassware using standard Schlenk, drybox techniques and anhydrous solvents. Dry dichloromethane (DCM), tetrahydrofuran (THF) and toluene were supplied by Durham Solvent Purification System, degassed and stored under nitrogen. The first generation ruthenium **12** and the second generation ruthenium complexes were purchased from Aldrich. 2,3,5,6-tetrafluoro-4-hydroxybenzoic acid was purchased from TCI Europe and used as supplied. Compound **13** [18], and ruthenium initiators **1a** [18], **14** [20] and **15** [10] were synthesized according to literature procedure.

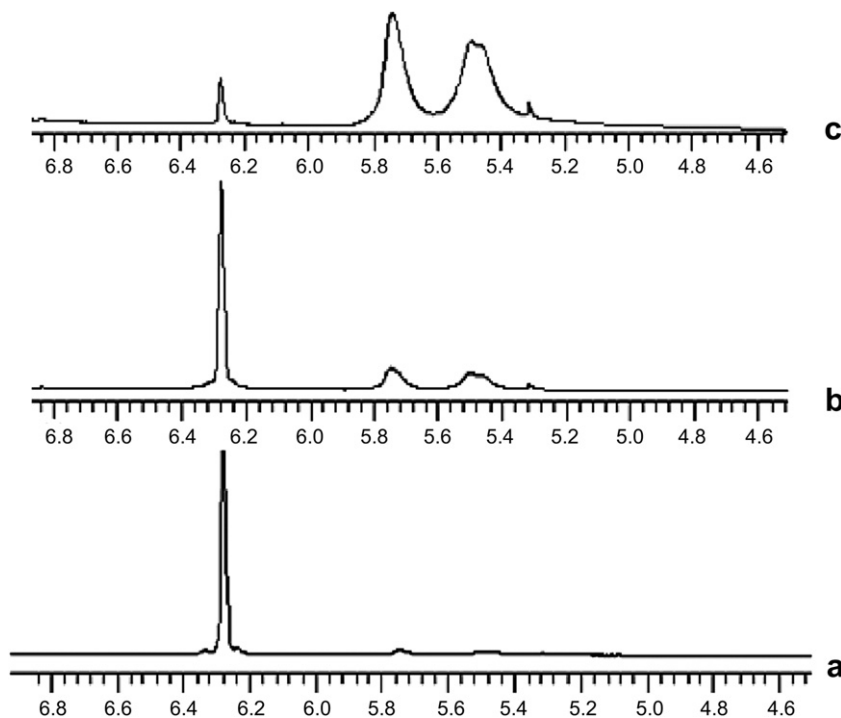


**Fig. 8.**  $^1\text{H}$  NMR spectra of the vinylic region for ROMP of HNB monomer with the new ruthenium initiator **9**: a) at room temperature after 1h; b) at 55 °C after 6 h; c) at 55 °C after 18 h.

N-2-ethylhexyl norbornene dicarboximide (2EHNB), N-hexyl norbornene dicarboximide (HNB), N-decyl norbornene dicarboximide (DecNB), N-Cyclohexyl norbornene dicarboximide (CyNB) and N-phenyl norbornene dicarboximide (PhNB) monomers were synthesized according to literature procedures [50,51].

The  $^1\text{H}$ ,  $^{13}\text{C}$  and  $^{31}\text{P}$  NMR spectra were recorded at room temperature on Bruker Avance 400 ( $^1\text{H}$ : 400.13,  $^{13}\text{C}$ : 100.61) or Varian Mercury 400 Spectrometers ( $^1\text{H}$ : 399.96,  $^{13}\text{C}$ : 100.98  $^{31}\text{P}$ : 161.91 and  $^{19}\text{F}$ : 376.29 MHz). All chemical shifts are reported in parts per million ( $\delta$ , ppm) with reference to  $\text{Me}_4\text{Si}$  (TMS,  $\delta$  0.0).

#### 4.2. Synthesis of thallium salt of methyl 2,3,5,6-tetrafluoro-4-hydroxybenzoate (**TI-6**)

To a solution of 2,3,5,6-tetrafluoro-4-hydroxybenzoic acid hydrate (5.2 g, 22.8 mmol) in methanol (400 ml) concentrated sulphuric acid (98%, 2 ml) was added. The solution was heated to reflux for 16 h. TLC was used to monitor the reaction. After the complete conversion, methanol was removed, and then water (100 ml) was added to the residual. Dichloromethane was used to extract the product from aqueous solution. The extract was dried over anhydrous magnesium sulphate, and the solvent was removed under reduced pressure to give white solid methyl 2,3,5,6-tetrafluoro-4-hydroxybenzoate (5.01 g, yield 90%).  $^1\text{H}$  NMR,  $\text{CD}_3\text{OD}$ : 4.92 (br s, 1H, OH), 3.92 (s, 3H,  $\text{COOCH}_3$ ).  $^{13}\text{C}$  NMR,  $\text{CD}_3\text{OD}$ : 162.7 (s, COO),

148.70–138.12 (m, Ar CF), 53.16 (s,  $\text{CH}_3$ ).  $^{19}\text{F}$  NMR,  $\text{CD}_3\text{OD}$ : –144.12 (m, 2F), –165.99 (m, 2F)

To a solution of methyl 2,3,5,6-tetrafluoro-4-hydroxybenzoate (1.02 g, 4.55 mmol) in anhydrous THF (10 ml) was added a solution of thallium ethoxide (1.19 g, 4.78 mmol, 1.05 eq) in anhydrous THF (5 ml). The white solid was formed and the suspension was stirred for further 3 h. The white solid was collected, washed with anhydrous THF, dried under reduced pressure, to give product **TI-6** (1.82 g, yield 90%).  $^1\text{H}$  NMR,  $\text{CD}_3\text{OD}$ : 3.92 (s, 3H,  $\text{COOCH}_3$ ).  $^{13}\text{C}$  NMR,  $\text{CD}_3\text{OD}$ : 162.7 (s, COO), 148.70–138.12 (m, Ar CF), 53.16 (s,  $\text{CH}_3$ ).  $^{19}\text{F}$  NMR,  $\text{CD}_3\text{OD}$ : –144.12 (m, 2F), –165.99 (m, 2F).

**Table 3**  
Summary of DSC results for the new ruthenium initiators **7–9** and **1a**.

Initiator	Monomer	DSC			
		Onset T, °C	Max. T, °C	Offset T, °C	Delta H, J/g
<b>7</b>	2EHNB	75	127	170	–119
<b>8</b>	HNB	60	100	125	–105
<b>1a</b>	HNB	40	55	65	

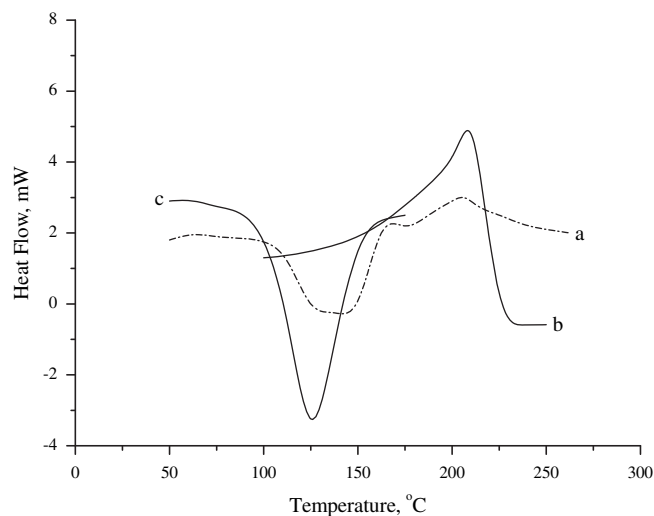


**Fig. 9.** DSC thermographs; (a) ROMP of 2EHNB monomer using initiator **7** run at 20–300 °C, (b) pure 2EHNB run at 20–300 °C, (c) ROMP of 2EHNB monomer using initiator **7** kept at 180 °C.

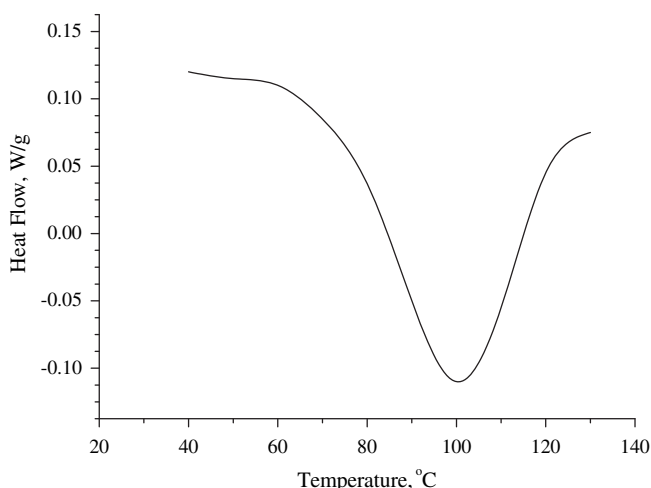


Fig. 10. DSC thermograph for ROMP of HNB monomer using ruthenium initiator **8**.

#### 4.3. Synthesis of new ruthenium initiator **7**

**Tl-6** (0.383 g, 0.90 mmol) and ruthenium complex **1a** (0.198 g, 0.44 mmol) were mixed in dichloromethane (5 ml) in a glove box. The resulting mixture was kept to stir overnight at ambient temperature. After the removal of the solid, the filtrate was reduced to dryness. Precipitation from dichloromethane–hexane afforded a brown powder product **7** (0.29 g, yield 80%).  $^1\text{H}$  NMR,  $\text{CD}_2\text{Cl}_2$ : 19.86 (t, 1H,  $[\text{Ru}]=\text{CH}$ ), 8.28 (d, 1H, pyridine), 7.48 (t, 1H, pyridine), 7.11 (d, 1H, pyridine), 6.96 (t, 1H, pyridine), 3.79 (s, 6H,  $\text{COOCH}_3$ ) 3.48 (t, 2H,  $=\text{CHCH}_2\text{CH}_2$ ), 2.52 (m, 5H,  $=\text{CHCH}_2\text{CH}_2$  and P( $\text{CHMe}_2$ )<sub>3</sub>), 1.34 (m, 18H, P( $\text{CHMe}_2$ )<sub>3</sub>).  $^{31}\text{P}$  NMR,  $\text{CD}_2\text{Cl}_2$ : 45.3.  $^{19}\text{F}$  NMR,  $\text{CDCl}_3$ : -145.19 (dd, 4F), -161.53 (t, 4F).

#### 4.4. Synthesis of ruthenium complex **11**

##### 4.4.1. Method A

In a glove box, ruthenium complex **1a** (0.045 g, 0.1 mmol) and tricyclohexylphosphine (2.8 g, 10 mmol) were mixed in dichloromethane (5 ml). The reaction was kept at room temperature for overnight. The volatiles were removed under reduced pressure and the residue triturated with hexanes. The solid was collected, washed with cold hexanes ( $3 \times 10$  ml) and dried under reduced pressure to give complex **11** as a pale green solid (0.033 g, yield 57%).

##### 4.4.2. Method B

In a glove box, compound **13** (4.0 g, 30 mmol) and ruthenium complex **12** (0.244 g, 0.3 mmol) were mixed in dichloromethane (5 ml) and the reaction was stirred at room temperature for 16 h. The volatiles were removed under reduced pressure and the residue triturated with hexanes. The solid was collected, washed with cold hexanes ( $3 \times 5$  ml) and dried under reduced pressure to give ruthenium complex **11** as a pale green solid (0.11 g, yield 65%).  $^1\text{H}$  NMR,  $\text{CDCl}_3$ : 17.75 (s, 1H,  $[\text{Ru}]=\text{CH}$ ), 7.48 (m, 2H, pyridine), 7.38 (m, 2H, pyridine), 2.97 (m, 4H,  $=\text{CHCH}_2\text{CH}_2$ ), 1.29 (m, 18H, P( $\text{C}_6\text{H}_{11}$ )<sub>3</sub>).  $^{31}\text{P}$  NMR,  $\text{CDCl}_3$ : 45.3.

#### 4.5. Synthesis of new ruthenium initiator **8**

**Tl-6** (0.122 g, 0.29 mmol) and ruthenium complex **11** (0.0813 g, 0.14 mmol) were mixed in dichloromethane (3 ml) in a glove box. The resulting mixture was stirred at ambient temperature for 16 h. The mixture was filtered and the filtrate was reduced to dryness

under reduced pressure. The resulting solid was washed with dichloromethane–hexane (1:5 v/v) to afford a brown powder product **8** (0.0862 g, yield 64%).  $^1\text{H}$  NMR,  $\text{CD}_2\text{Cl}_2$ : 19.91 (t, 1H,  $[\text{Ru}]=\text{CH}$ ), 8.54 (d, 1H, pyridine), 7.68 (t, 1H, pyridine), 7.22 (m, 2H, pyridine), 3.87 (s, 6H,  $\text{COOCH}_3$ ) 3.48 (t, 2H,  $=\text{CHCH}_2\text{CH}_2$ ), 2.28 (m, 5H,  $=\text{CHCH}_2\text{CH}_2$  and P( $\text{CHMe}_2$ )<sub>3</sub>), 1.32 (m, 18H, P( $\text{CHMe}_2$ )<sub>3</sub>).  $^{31}\text{P}$  NMR,  $\text{CD}_2\text{Cl}_2$ : 45.3.  $^{19}\text{F}$  NMR,  $\text{CDCl}_3$ : -145.19 (dd, 4F), -161.53 (t, 4F).

#### 4.6. Synthesis of new ruthenium initiator **9**

**Tl-6** (0.095 g, 0.22 mmol) and ruthenium complex **14** (0.066 g, 0.11 mmol) were mixed in dichloromethane (3 ml) in a glove box. The resulting mixture was stirred at ambient temperature for 16 h. The mixture was filtered and the filtrate was reduced to dryness under reduced pressure. The resulting solid was washed with dichloromethane–hexane (1:5 v/v) to afford a green powder product **9** (0.0704 g, yield 66%).  $^1\text{H}$  NMR,  $\text{CDCl}_3$ : 19.47 (t, 1H,  $[\text{Ru}]=\text{CH}$ ), 7.82 (d, 1H, pyridine), 7.35 (td, 1H, pyridine), 7.21 (d, 1H, pyridine), 6.94 (d, 4H, Mes), 6.82 (td, 1H, pyridine), 4.06 (s, 4H, sIMes), 3.83 (s, 2H,  $=\text{CHCH}_2\text{CH}_2$ ), 3.79 (s, 6H,  $\text{COOCH}_3$ ), 2.41 (s, 12H, Mes  $\text{CH}_3$ ), 2.27 (s, 6H, Mes  $\text{CH}_3$ ), 1.70 (d, 2H,  $=\text{CHCH}_2\text{CH}_2$ ).  $^{19}\text{F}$  NMR,  $\text{CDCl}_3$ : -145.19 (dd, 4F), -161.53 (t, 4F).

#### 4.7. Synthesis of new ruthenium complex **10**

**Tl-6** (0.218 g, 0.51 mmol) and ruthenium complex **15** (0.218 g, 0.25 mmol) were mixed in dichloromethane (5 ml) in a glove box. The resulting mixture was stirred at ambient temperature for 16 h. The mixture was filtered and the filtrate was reduced to dryness under reduced pressure. The resulting solid was washed with dichloromethane–hexane (1:5 v/v) to afford a green powder product **10** (0.21 g, yield 77%).  $^1\text{H}$  NMR,  $\text{CD}_2\text{Cl}_2$ : 18.77 (s, 1H,  $[\text{Ru}]=\text{CH}$ ), 7.93 (d, 1H, pyridine), 7.69 (m, 1H, pyridine), 7.67 (m, 1H, Ph CH), 7.47 (m, 1H, pyridine), 7.28 (d, 2H, Ph CH), 7.22 (br. s, 2H, Ph CH), 7.13–7.09 (t, 2H, Mes CH), 6.79 (s, 1H, pyridine), 6.76 (m, 2H, Ph, Mes CH), 4.07 (m, 4H, sIMes), 3.77 (s, 3H,  $\text{COOCH}_3$ ), 3.69 (s, 3H,  $\text{COOCH}_3$ ), 2.57 (s, 6H, Mes  $\text{CH}_3$ ), 2.41 (s, 6H, Mes  $\text{CH}_3$ ), 1.82 (s, 6H, Mes  $\text{CH}_3$ ).  $^{19}\text{F}$  NMR,  $\text{CDCl}_3$ : -145.19 (dd, 4F), -161.53 (t, 4F).

#### 4.8. ROMP reactions for solution $^1\text{H}$ NMR experiments

All solution  $^1\text{H}$  NMR experiments were carried out at a monomer to initiator ratio of 20:1 in NMR tubes equipped with Young's tap. In a typical reaction the ruthenium initiator (10 mg) was weighed into a sample vial and dissolved in  $\text{CDCl}_3$  (0.4 ml). Norbornene dicarboximide monomer was weighed into another sample vial and  $\text{CDCl}_3$  (0.5 ml) was added. The vial containing monomer was added to the vial containing initiator and the mixture stirred for 5 min. The reaction mixture was transferred into an NMR tube. The reactions were carried out at room temperature and at 55 °C. The course of the reactions was followed by  $^1\text{H}$  NMR.

#### 4.9. ROMP reactions for DSC experiments

All ROMP reactions for DSC experiments were carried out at a monomer to initiator ratio of 50:1. The catalysts was weighed into the mixing vessel and dissolved in a minimum of deuterated chloroform (5 drops). The monomer was added and mixed by dual asymmetric centrifuge (DAC) mixer for 5 min. The sample was then placed in a vacuum chamber, equipped with an Edward 5 Vacuum pump, at room temperature for 30 min to ensure all solvent was removed. Approx. 5 mg of the material was transferred into a standard Perkin–Elmer pan. The open pan was then placed into the TA Instruments Q100 DSC System. Specimens were heated from 25 °C to 300 °C at a rate of 10 °C/min in a nitrogen atmosphere.

**Table 4**  
Crystal data and X-ray experiment details.

Compound	10	7
Empirical formula	C <sub>49</sub> H <sub>42</sub> BrF <sub>8</sub> N <sub>3</sub> O <sub>6</sub> Ru · ½CH <sub>2</sub> Cl <sub>2</sub>	C <sub>33</sub> H <sub>36</sub> F <sub>8</sub> NO <sub>6</sub> PRu
Formula weight	1144.30	826.67
T, K	120	120
Crystal system	Monoclinic	Triclinic
Space group (No.)	P2 <sub>1</sub> /c (# 14)	P-1 (# 2)
a, Å	21.027(2)	9.9036(10)
b, Å	20.353(2)	11.1367(11)
c, Å	23.900(2)	16.1893(15)
α, °	90	89.72(1)
β, °	112.78(1)	82.75(1)
γ, °	90	82.52(1)
V, Å <sup>3</sup>	9431(1)	1756.1(3)
Z	8	2
ρ (calc.), g/cm <sup>3</sup>	1.612	1.563
μ (Mo Kα), mm <sup>-1</sup>	1.32	0.58
Reflections collected	111,493	20,920
Independent reflections	24,998	9281
R(int)	0.051	0.045
R [I > 2σ(I)]	0.038	0.048
wR(F <sup>2</sup> ) [all data]	0.090	0.101

#### 4.10. X-ray crystallography

Experiments (Table 4) were carried out on a Siemens 3-circle diffractometer with a SMART 1000 CCD area detector, using graphite-monochromated Mo Kα radiation ( $\lambda = 0.71073 \text{ \AA}$ ) and a Cryostream (Oxford Cryosystems) open-flow N<sub>2</sub> cryostat. Diffraction data were measured using 0.3° ω-scans and corrected for absorption by Gaussian integration based on crystal face-indexing [52]. The structures were solved by direct methods and refined by full-matrix least squares against F<sup>2</sup> of all reflections, using SHELXTL software [53].

#### Acknowledgements

We thank ICI for their financial support of the project. We also thank Mr. Douglas Carswell for performing the thermal analyses.

#### Appendix A. Supplementary material

CCDC 751991 for **10** ½CH<sub>2</sub>Cl<sub>2</sub>, and 751992 for **7** contain the supplementary crystallographic data for this paper. These data can be obtained free of charge from The Cambridge Crystallographic Data Center via [www.ccdc.cam.ac.uk/data\\_request/cif](http://www.ccdc.cam.ac.uk/data_request/cif).

#### References

- [1] R.R. Schrock, R.T. DePue, J. Feldman, C.J. Schaverien, J.C. Dewan, A.H. Liu, J. Am. Chem. Soc. 110 (2002) 1423–1435.
- [2] J.S. Murdzek, R.R. Schrock, Organometallics 6 (2002) 1373–1374.
- [3] G.C. Bazan, E. Khosravi, R.R. Schrock, W.J. Feast, V.C. Gibson, M.B. O'Regan, J.K. Thomas, W.M. Davis, J. Am. Chem. Soc. 112 (2002) 8378–8387.
- [4] R.R. Schrock, Chem. Rev. 109 (2009) 3211–3226.
- [5] W.J. Feast, E. Khosravi, J. Fluorine Chem. 100 (1999) 117–125.
- [6] P. Schwab, R.H. Grubbs, J.W. Ziller, J. Am. Chem. Soc. 118 (1996) 100–110.

- [7] C.W. Bie1awski, R.H. Grubbs, Angew. Chem. 112 (2000) 3025–3028.
- [8] C. Samojlowicz, M. Bieniek, K. Grela, Chem. Rev. 109 (2009) 3708–3742.
- [9] D.M. Haigh, A.M. Kenwright, E. Khosravi, Tetrahedron 60 (2004) 7217–7224.
- [10] J.A. Love, J.P. Morgan, T.M. Trnka, R.H. Grubbs, Angew. Chem. Int. Ed. 41 (2002) 4035–4037.
- [11] T.C. Castle, E. Khosravi, L.R. Hutchings, Macromolecules 39 (2006) 5639–5645.
- [12] A.M. Tayer, Chem. Eng. News (February 12, 2007) 37–47.
- [13] T.C. Castle, L.R. Hutchings, E. Khosravi, Macromolecules 37 (2004) 2035–2040.
- [14] I. Czelusniak, E. Khosravi, A.M. Kenwright, C.W.G. Ansell, Macromolecules 40 (2007) 1444–1452.
- [15] R.H. Grubbs, Handbook of Metathesis, Wiley-VCH, Weinheim, Germany, 2003.
- [16] C. Slugovc, Macromol. Rapid Commun. 25 (2004) 1283–1297.
- [17] A. Leitgeb, J. Wappel, C. Slugovc, Polymer 51 (2010) 2927–2946.
- [18] P.A. van der Schaaf, R. Kolly, H.-J. Kirner, F. Rime, A. Muhlebach, A. Hafner, J. Organomet. Chem. 606 (2000) 65–74.
- [19] P.A. van der Schaaf, A. Muhlebach, A. Hafner, WO 99/00397.
- [20] T. Ung, A. Hejl, R.H. Grubbs, Y. Schrodi, Organometallics 23 (2004) 5399–5401.
- [21] A. Hejl, M.W. Day, R.H. Grubbs, Organometallics 25 (2006) 6149–6154.
- [22] X. Gstrein, D. Burtscher, A. Szadkowska, M. Barbasiewicz, F. Stelzer, K. Grela, C. Slugovc, J. Polym. Sci. Part A Polym. Chem. 45 (2007) 3494–3500.
- [23] C. Slugovc, D. Burtscher, F. Stelzer, K. Mereiter, Organometallics 24 (2005) 2255–2258.
- [24] B. De Clercq, F. Verpoort, Tetrahedron Lett. 43 (2002) 9101–9104.
- [25] K. Denk, J. Fridgen, W.A. Herrmann, Adv. Synth. Catal. 344 (2002) 666–670.
- [26] J. Louie, R.H. Grubbs, Organometallics 21 (2002) 2153–2164.
- [27] A. Szadkowska, K. Grela, Curr. Org. Chem. 12 (2008) 1631–1647.
- [28] S. Monsaert, A. Lozano Vila, R. Drozdak, P. Van Der Voort, F. Verpoort, Chem. Soc. Rev. 38 (2009) 3360–3372.
- [29] A. Muhlebach, P.A. van der Schaaf, A. Hafner, R. Kolly, F. Rime, H.-J. Kirner, Ring opening metathesis polymerization and related chemistry. in: E. Khosravi, T. Szymanska Buzar (Eds.), Nato Science Series. Kluwer Academic Publishers, 2002, pp. 23–44.
- [30] J.S. Kingsbury, J.P.A. Harrity, P.J. Bonitatebus, A.H. Hoveyda, J. Am. Chem. Soc. 121 (1999) 791–799.
- [31] S.B. Garber, J.S. Kingsbury, B.L. Gray, A.H. Hoveyda, J. Am. Chem. Soc. 122 (2000) 8168–8179.
- [32] S. Gessler, S. Randl, S. Blechert, Tetrahedron Lett. 41 (2000) 9973–9976.
- [33] A.H. Hoveyda, D.G. Gillingham, J.J. Van Veldhuizen, O. Kataoka, S.B. Garber, J.S. Kingsbury, J.P.A. Harrity, Org. Biomol. Chem. 2 (2004) 8–23.
- [34] M. Barbasiewicz, A. Szadkowska, A. Makal, K. Jarzemska, K. Wozniak, K. Grela, Chem. Eur. J. 14 (2008) 9330–9337.
- [35] X. Solans-Monfort, R. Pleixats, M. Sodupe, Chem. Eur. J. 16 (2010) 7331–7343.
- [36] J.C. Conrad, D. Amoroso, P. Czechura, G.P.A. Yap, D.E. Fogg, Organometallics 22 (2003) 3634–3636.
- [37] J.C. Conrad, J.L. Snelgrove, M.D. Eelman, S. Hall, D.E. Fogg, J. Mol. Catal. A Chem. 254 (2006) 105–110.
- [38] J.C. Conrad, K.D. Camm, D.E. Fogg, Inorg. Chim. Acta 359 (2006) 1967–1973.
- [39] S. Monfette, D.E. Fogg, Organometallics 25 (2006) 1940–1944.
- [40] A. Michrowska, R. Bujok, S. Harutyunyan, V. Sashuk, G. Dolgonos, K. Grela, J. Am. Chem. Soc. 126 (2004) 9318–9325.
- [41] L. Gulajski, A. Michrowska, R. Bujok, K. Grela, J. Mol. Catal. A Chem. 254 (2006) 118–123.
- [42] M.S. Sanford, J.A. Love, R.H. Grubbs, J. Am. Chem. Soc. 123 (2001) 6543–6554.
- [43] G.C. Vougioukalakis, R.H. Grubbs, Chem. Eur. J. 14 (2008) 7545–7556.
- [44] T. Vorfalt, K.-J. Wannowius, H. Plenio, Angew. Chem. Int. Ed. 49 (2010) 5533–5536.
- [45] A. Furstner, P.W. Davies, C.W. Lehmann, Organometallics 24 (2005) 4065–4071.
- [46] S. Nag, K. Banerjee, D. Datta, New J. Chem. 31 (2007) 832–834.
- [47] S.S. Batsanov, Inorg. Mater. 37 (2001) 871.
- [48] R.S. Rowland, R. Taylor, J. Phys. Chem. 100 (1996) 7384–7391.
- [49] M.W. Day, J.A. Love, R.H. Grubbs, Private communication to Cambridge Structural Database, CCDC-191510 (2005) ref. code NALTIE.
- [50] E. Khosravi, A.A. Al-Hajaji, Eur. Polym. J. 34 (1998) 153–157.
- [51] P.J. Hine, T. Leejarkpai, E. Khosravi, R.A. Duckett, W.J. Feast, Polymer 42 (2001) 9413–9422.
- [52] G.M. Sheldrick, SADABS 2006/1, Bruker–Nonius AXS, Madison, Wisconsin, USA.
- [53] G.M. Sheldrick, SHELXTL, Version 6.14. Bruker–Nonius AXS, Madison, Wisconsin, USA, 2003.